Intrinsic connectivity networks in posterior cortical atrophy: A role for the pulvinar?

Carolyn A. Fredericks[*],[1], Jesse A. Brown, Jersey Deng, Abigail Kramer, Rik Ossenkoppele[2], Katherine Rankin, Joel H. Kramer, Bruce L. Miller, Gil D. Rabinovici, William W. Seeley

Memory and Aging Center, University of California, 675 Nelson Rising Lane, San Francisco, CA 94143, USA

ARTICLE INFO

ABSTRACT

Background: Posterior cortical atrophy (PCA) is a clinical variant of Alzheimer's disease (AD) that presents with progressive visuospatial symptoms. While amnestic AD is characterized by disrupted default mode network (DMN) connectivity with corresponding increases in salience network (SN) connectivity, a visuospatial network appears to be disrupted early in PCA. Based on PCA patients' clinical features, we hypothesized that, in addition to early decreased integrity within the visuospatial network, patients with PCA would show increases in SN connectivity despite relative preservation of DMN. As the lateral pulvinar nucleus of the thalamus has direct anatomical connections with striate and extrastriate cortex and DMN, and the medial pulvinar is anatomically interconnected with SN, we further hypothesized that lateral and medial pulvinar nuclei might be implicated in intrinsic connectivity changes in PCA.

Methods: 26 patients with PCA and 64 matched controls were recruited through UCSF Memory and Aging Center research programs. Each completed a standardized neuropsychological battery, structural MRI, and task-free fMRI. Seed-based functional correlations were used to probe networks of interest, including those seeded by the medial and lateral pulvinar thalamic nuclei, across the whole brain, and functional data analyses were adjusted for brain atrophy.

Results: Patients with PCA showed disproportionate deficits in the visuospatial domain; they also showed preserved social sensitivity and endorsed more depressive symptoms than HCs. PCA patients had significant parietooccipital atrophy accompanied by widespread connectivity decreases within the visuospatial network, enhanced connectivity between some structures in SN, and enhanced connectivity between key nodes of the DMN compared to controls. Increased SN connectivity correlated with a measure of social sensitivity, and increased DMN connectivity correlated with short-term memory performance. Medial pulvinar connectivity increases in PCA were topographically similar to SN (anterior insula) connectivity increases, while lateral pulvinar connectivity increases were similar to DMN (posterior cingulate) connectivity increases.

Conclusions: PCA is characterized by preserved to heightened connectivity in the SN and DMN despite decreased visuospatial network connectivity. The spatial similarity of medial and lateral pulvinar connectivity changes to those seen in the SN and DMN suggests a role for the pulvinar in intrinsic connectivity network changes in PCA.

1. Introduction

Posterior cortical atrophy (PCA) is an uncommon Alzheimer's disease (AD) syndromic variant presenting with progressive visual and visuospatial symptoms and early parietooccipital atrophy (Benson et al., 1988; Crutch et al., 2017; Mendez et al., 2002). Imaging studies suggest that a parietooccipital visuospatial network is the critical vulnerable network in patients with PCA. Identifying the point of peak atrophy in a group of patients with PCA, then using it as a seed in healthy controls (HCs), elicits this visuospatial network (Lehmann et al., 2013), and connectivity within the network is lower in PCA patients compared with patients with other AD variants (Lehmann et al., 2015). Amnestic symptoms, on the other hand, are less prominent in patients with PCA than those with amnestic AD, and structures critical for supporting episodic memory, such as the hippocampus, atrophy later than visuospatial structures (Ossenkoppele et al., 2015). At autopsy, the same pattern holds: patients with PCA show a higher burden of tau pathology in striate and extrastriate cortex relative to the medial temporal lobe (Tang-Wai et al., 2004; Hof et al., 1993).

In terms of large-scale functional networks, amnestic AD is characterized by disrupted connectivity in the default mode network (DMN), which supports episodic memory, with corresponding increased connectivity in a salience network (SN) (Zhou et al., 2010; Greicius et al., 2004; Mormino et al., 2011; Rabinovici et al., 2007), which is critical for socially adaptive behavior (Seeley et al., 2012). Increased SN connectivity correlates with neuropsychiatric symptoms in amnestic AD patients (Balthazar et al., 2014), who, despite their prominent episodic memory symptoms, show preserved empathic concern for others and greater personal distress and depressive symptoms compared with healthy controls (Sturm et al., 2013). Patients with early-stage PCA, too, remain socially sensitive, often to the point of clinical anxiety (Benson et al., 1988), which may be even more common in PCA than in amnestic AD (Isella et al., 2015). However, little is known about how PCA affects functional networks outside of the visuospatial network. We hypothesized that, in addition to showing early decreased integrity within the visuospatial network, PCA patients would show increases in SN connectivity (correlating with preserved socioemotional function and increased emotional reactivity) despite relative preservation of DMN (correlating with milder amnestic symptoms relative to amnestic AD).

Considering these hypothesized relationships between large-scale functional networks, we questioned which structures might mediate increases in SN connectivity despite decreased visuospatial network integrity. Thalamic nuclei are electrophysiologically and anatomically well-positioned to regulate network coherence and to serve as network switches (Hwang et al., 2017; Bell & Shine, 2016; Sherman, 2016), and an emerging literature links thalamic pathology to increased thalamocortical and thalamolimbic activity in animal models of AD (Hazra et al., 2016). We became interested, therefore, in the role that thalamic nuclei might play in network binding in PCA. Because the lateral pulvinar's projections target striate and extrastriate cortex, as well as several key nodes of the DMN, (Benarroch, 2015; Robinson & Petersen, 1992; Yeterian & Pandya, 1995), while the medial pulvinar has prominent reciprocal connections with orbitofrontal, parahippocampal, cingulate, insular and amygdalar regions (Benarroch, 2015; Jones & Burton, 1976; Mufson & Mesulam, 1984; Romanski et al., 1997), major nodes of SN (Seeley et al., 2007), we focused our attention on the lateral and medial pulvinar nuclei. We hypothesized that lateral pulvinar connectivity would recapitulate visuospatial network connectivity, showing significant decreases in PCA, while medial pulvinar connectivity would recapitulate SN connectivity, showing significant increases in PCA. To evaluate these hypotheses, we performed neuropsychological testing and evaluated structural and functional connectivity in individuals with PCA and matched HCs.

2. Material and methods

2.1. Participants

26 individuals diagnosed with PCA based on Mendez criteria (Mendez et al., 2002) and 64 matched controls were recruited through UCSF Memory and Aging Center research programs. Of the individuals with a diagnosis of PCA, 22 were amyloid PET-positive; one of the remaining four had a pathologic diagnosis of AD (graded A2, B3, C3), and the remaining three opted not to undergo amyloid PET. Each participant completed a medical history and physical examination, standardized neuropsychological battery, structural imaging, and task-free fMRI. For the PCA group, individuals were excluded from study if they met core clinical criteria for another neurodegenerative syndrome (such as corticobasal syndrome (Armstrong et al., 2013) or Lewy body disease (McKeith et al., 2017)), had clinically significant cerebrovascular disease, met criteria for other major neurologic or systemic illness, or were taking medications which could significantly impact cognitive function. For HCs, additional exclusion criteria included abnormal performance on cognitive screening. All study procedures were approved by the institutional review board of the University of California, San Francisco, and all subjects or their assigned surrogate decision-makers provided informed consent prior to participation.

PCA patients were well-matched with the control group by age, handedness, gender, years of education, and presence of the ApoE ε4 allele (Table 1).

2.2. Neuropsychological assessment

All participants underwent a standardized neuropsychological battery within 180 days of imaging to evaluate cognitive functioning, consisting of assessments of global functioning, verbal memory, visuospatial functioning, language, and executive functioning. PCA and HC groups were compared in each of these domains. Global functioning was measured using the Mini Mental State Exam (MMSE (Folstein et al., 1975)). Verbal memory performance was assessed using the z- score for long delay recall on the California Verbal Learning Test-II (CVLT-II, 16 items) or CVLT-Short Form (9 items) (Delis et al., 2000). To evaluate visuospatial performance, a composite z-score for each participant was created by averaging z-scores for his or her scores on the Benson figure copy (Possin et al., 2011) and Number Location subtest of the Visual Object and Space Perception Battery (Warrington, 1991). Similarly, a language composite z-score was created for each participant by averaging his or her z-scores for semantic fluency (animal naming (Weintraub et al., 2009)) and abbreviated form of the Boston Naming Test (aBNT) (Mack et al., 1992) scores. Lastly, an executive function composite z-score was created by averaging phonemic fluency (D-words) (Spreen & Strauss, 1998) and digits backward (Weschler, 1987) scores.

To evaluate for between-group differences in social sensitivity, we used the Interpersonal Reactivity Index (IRI) (Davis, 1983), which

Table 1

Demographics of PCA patients and healthy controls.

	PCA, $n = 26$	HC, $n = 64$	p	n
Age, mean (SD)	62.12 (7.98)	62.55 (7.57)	0.81	90
Handedness, % left	11.54%	12.50%	0.90	90
Gender, % female	53.85%	53.13%	0.95	90
Edu, mean (SD)	16.19 (3.73)	16.42 (1.91)	0.70	90
ApoE ε4, % pos	37.50%	32.81%	0.68	88
MMSE, 30-point mean (SD)	22.87 (5.29)	29.60 (0.56)	< 0.001	87
VOSP, 10-item mean (SD)	2.42 (3.01)	9.25 (0.94)	< 0.001	85
Benson Fig. Copy, 17-point mean (SD)	3.42 (4.02)	15.39 (0.90)	< 0.001	80
CDR sum of boxes mean (SD)	4.44 (1.86)	0 (0)	< 0.001	90

includes measures of empathic concern, cognitive perspective-taking, and personal distress during upsetting situations, and the Geriatric Depression Scale (GDS) (Yesavage et al., 1982), which screens for depressive symptoms.

Between-group demographic variables were compared using Student's t-test and chi-square tests as appropriate. For cognitive testing analyses, each individual's z-scores for each cognitive domain were entered into a general linear model, controlling for gender, age, and education. To test the hypothesis that PCA patients performed significantly worse than HCs in all domains and more so in the visuospatial domain, we calculated F-scores for between-group performance in each domain. Paired samples t-tests within the PCA group were used to compare PCA patients' performance between domains. We used two-sample t-tests to compare GDS and IRI performance between PCA and HC groups. Subjects with missing data were excluded case-wise from analyses.

2.3. Image acquisition and preprocessing

All participants underwent MRI at the UCSF Neuroscience Imaging Center. Images were acquired on a 3 T Siemens Tim Trio system equipped with a 12-channel head coil. T1-weighted structural images were acquired using a volumetric MPRAGE sequence ($1 \times 1 \times 1$ mm voxel size; FOV = 256×240 mm and 160 slices, TR = 2300 ms, TE = 3 ms, FA = 9°). Task-free fMRI was acquired over an 8-min sequence during which participants were instructed to remain awake with their eyes closed ($2.5 \times 2.5 \times 3$ mm voxel size; FOV = 230×230 mm, TE = 27 ms, TR = 2 s, FA = 80°, 36 interleaved axial slices).

Preprocessing for fMRI images was conducted in SPM12 (http://www.fil.ion.ucl.ac.uk/spm/software/spm12/) and FSL (where specified; http://fsl.fmrib.ox.ac.uk/fsl). After discarding the first five volumes, the remaining 235 volumes were slice-time corrected, realigned to the mean functional image, and assessed for motion (both rotational and translational). Volumes were coregistered to each individual's MPRAGE image, and SPM segment was then used to normalize them to the standard SPM healthy adult tissue probability template at an isotropic resolution of 2 mm³. They were then smoothed with a 6 mm Gaussian kernel and band-pass filtered in the 0.008–0.15 Hz frequency range using fslmaths. Nuisance parameters for CSF and white matter were estimated using a mask located in the center of the lateral ventricles and a mask of the highest probability cortical white matter (as derived by FSL tissue prior mask). Additional nuisance parameters included the 3 translational and 3 rotational motion parameters, the temporal derivatives of the previous 8 terms, and the squares of the previous 16 terms (Satterthwaite et al., 2013). The same band-pass filter applied to volumes above was applied to these nuisance data in order to avoid reintroduction of noise. Inclusion criteria for head motion included maximum relative head motion < 3 mm, maximum relative rotation < 3°, and the maximum number of motion spikes (relative motion > 1 mm) < 10% of the total number of frames.

2.4. Image analysis

We assessed structural atrophy using whole-brain voxel-based morphometry (VBM) in SPM12. Images were normalized as described in the previous section, modulated, and spatially smoothed with an 8 mm kernel. Between-group differences were assessed by two-sample t-test via SPM12's general linear model framework. Nuisance covariates included age, sex, handedness, and education.

Task-free fMRI scans were analyzed by calculating average voxel-wise time series from seeds for networks of interest. Five seeds, for the visuospatial network, SN, DMN, and medial and lateral pulvinar nucleus (Fig. 1), were derived as follows:

Visuospatial Network: We seeded the visuospatial network using a 4 mm radius spherical seed surrounding the peak atrophy point from a prior independent study of individuals with PCA (right middle occipital gyrus, 39, −88, 10 in MNI space) (Ossenkoppele et al., 2015). This seed was shown to produce the visuospatial network when used as a seed in a group of healthy controls (Lehmann et al., 2013).

SN: We chose a R anterior insula seed to elicit SN. This seed was previously derived by our group via an activation likelihood estimate meta-analysis of socio-emotional task-based fMRI studies that activate the insula in healthy controls (Guo et al., 2012).

DMN: We used a R posterior cingulate seed, derived by placing a 4 mm radius spherical seed at the center of gravity of a cluster previously identified in this region by our group in a separate sample of HCs (Gardner et al., 2013), to elicit DMN.

Medial and Lateral Pulvinar Thalamus: Seeds for the medial and lateral pulvinar were derived from a non-overlapping matched group of healthy controls ($n = 98$, mean age = 63.08). We used the salience and ventral visual networks from a robust, previously published 17-network cortical parcellation (Yeo et al., 2011) and assessed which voxels within the pulvinar had time series that correlated best with SN versus the ventral visual network (yielding bilateral medial pulvinar clusters) and with the ventral visual network versus SN (yielding bilateral lateral pulvinar clusters). We then placed 2 mm radius spherical seeds at the center of mass of these medial and lateral pulvinar clusters. Please see Supplemental Methods for details.

Seeds for each network were then used as covariates of interest in a whole-brain, linear regression, statistical parametric analysis to generate a map scoring each voxel in the brain based on its correlation with the seed ROI, controlling for the aforementioned nuisance parameters. Resultant data from each subject were fitted to a second-level regression model for group random effects analysis. Functional data analyses were atrophy-corrected using the BPM toolbox (Casanova et al., 2007). All maps were thresholded at a joint height and extent probability threshold of $p < .05$, corrected at the whole brain level. After noting similarities between thresholded whole brain maps of pulvinar connectivity and SN/DMN connectivity, we conducted post-hoc analyses quantifying the overlap of each pair of maps using Sørenson-Dice coefficients. Sørenson-Dice coefficients were calculated as two times the number of overlapping voxels between thresholded maps divided by the sum of the number of voxels in thresholded maps one and two.

To assess for relationships between neuropsychological variables and clusters identified as significantly different between patients with PCA and HCs in the analyses above, we conducted post-hoc exploratory analyses evaluating Spearman rank-order correlations between (Benson et al., 1988) VOSP score and visuospatial network integrity, (Crutch et al., 2017) CVLT long recall (memory performance) and DMN integrity, and (Mendez et al., 2002) IRI (empathic concern and personal distress) and SN integrity in patients with PCA. Mean connectivity values for clusters of interest from the maps described above (a parietooccipital cluster whose connectivity to the visual atrophy seed was significantly decreased for PCA patients vs HCs; a bilateral angular gyrus cluster whose connectivity to R posterior cingulate was significantly increased for PCA patients vs HCs; and medial prefrontal and ventral striatal clusters whose connectivity to R frontoinsula was significantly increased for PCA patients vs HCs) were derived for each subject (Fig. 7). For each cluster of interest, to ensure that observed relative increases for one group compared to the other reflected true increases in connectivity, rather than loss of anticorrelation, we examined mean connectivity values (representing average correlation coefficients from all voxels within each cluster to the relevant network seed) in PCA patients and HCs. For each of the four clusters, correlation coefficients were positive within at least one standard deviation from the mean in both PCA patients and HCs. To ensure that the four clusters included only gray matter, we applied a post-hoc probabilistic gray matter map; all voxels within each cluster were gray matter. All correlations were corrected for average gray matter atrophy for each cluster for each participant.
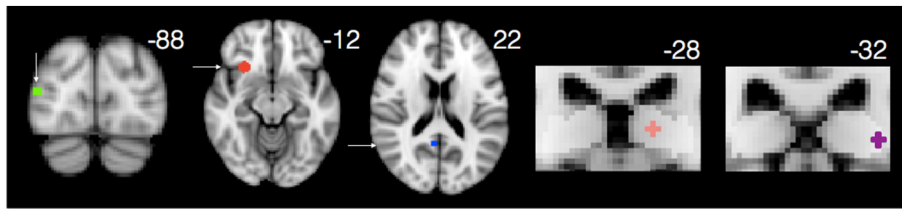
3. Results

3.1. PCA patients have disproportionate deficits on tests of visuospatial function

As anticipated, individuals with PCA performed significantly worse than controls on a measure of global cognitive function (MMSE, F = 75.632, $p < .005$). They also performed significantly worse across cognitive domains (Executive Function: F = 82.798, p < .005, Language: F = 71.536, p < .005, Memory: F = 89.712, p < .005), with worst performance in the visuospatial domain (F = 388.879, p < .005). Within the PCA subject group, visuospatial deficits were significantly worse than deficits in memory ($t = -10.710$, p < .005), language ($t = -9.376$, p < .005), or executive function ($t = -13.187$, p < .005) (Fig. 2).

3.2. PCA patients show preserved social sensitivity and report more depressive symptoms

Individuals with PCA showed preserved empathic concern ($t = 0.44$, $p = .66$) and cognitive perspective-taking ($t = 0.75$, $p = .45$) when compared with HCs, but had increased levels of personal distress ($t = 3.45$, $p = .001$). Despite both groups scoring within the normal range on depression screen (0–9), PCA patients scored significantly higher than HCs ($t = 5.52$, $p < .001$) (Fig. 3).

3.3. PCA patients have significant parietooccipital atrophy with corresponding decreased connectivity within the visuospatial network

Consistent with past studies, VBM revealed marked parietooccipital atrophy in individuals with PCA compared with HCs, even at a stringent voxelwise threshold of $t > 10$ (Fig. 4A). The point of peak atrophy was located at midline precuneus (2, −63, 38).

Individuals with PCA showed widespread decreased connectivity within the visuospatial network compared with HCs (Ossenkoppele
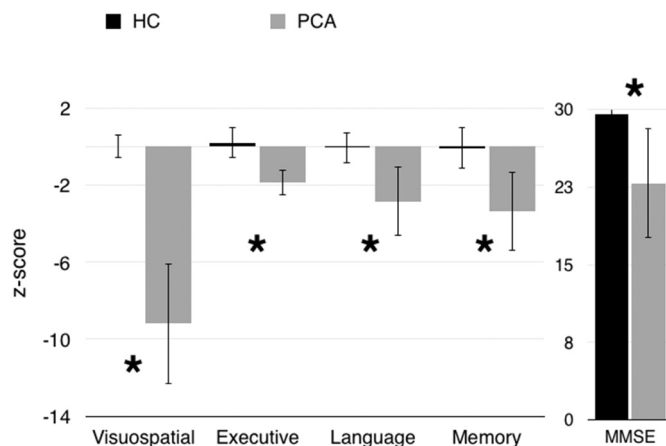

Fig. 2. Z-scores across cognitive domains, and raw MMSE scores, were significantly worse in the PCA group than the HC group, and visuospatial function was disproportionately affected. Error bars represent standard deviation. (*p < .005).
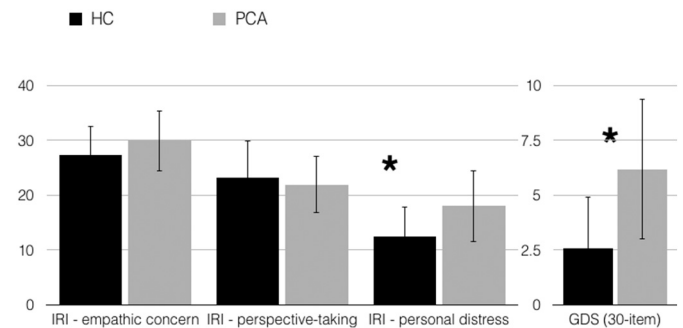

Fig. 3. Individuals with PCA showed preserved empathic concern and cognitive perspective-taking; they had increased levels of personal distress and scored higher than HCs on a measure of depressive symptoms. Error bars represent standard deviation. (*$p \leq .001$).

et al., 2015). They also showed decreased connectivity between the network seed and bilateral insula and prefrontal cortex. Interestingly, they showed increased connectivity between this region and the right angular gyrus, a major node within the DMN, despite significant atrophy in this area (Fig. 4B).

3.4. PCA patients show increased connectivity within key nodes of SN and DMN

From the right anterior insula SN seed, PCA patients showed increased connectivity to ventromedial prefrontal cortex and nucleus accumbens but decreased connectivity to the bilateral insula. They also showed decreased out-of-network connectivity from the seed to parietooccipital cortex (Fig. 5A). From the DMN seed, they showed increased connectivity between key nodes of the DMN, including anterior cingulate, precuneus, and angular gyrus, compared to controls, but decreased connectivity to right hippocampus (Fig. 5B). They showed widespread decreased out-of-network connectivity throughout other parietal regions, occipital cortex, insula, and dorsal frontal structures.

3.5. Medial pulvinar connectivity mirrors SN, while lateral pulvinar connectivity mirrors DMN

Regions where PCA patients showed relative increases in medial pulvinar connectivity (Fig. 5C) were strikingly similar to regions of SN connectivity increases (right frontoinsular seed, Fig. 5A), with overlapping clusters in ventromedial PFC and left accumbens (Dice coefficient 0.16, Fig. 6A). Regions where PCA patients showed increases in lateral pulvinar connectivity (Fig. 5D) were strikingly similar to regions of increases in DMN connectivity (right posterior cingulate seed, Fig. 5B), with overlapping clusters in bilateral angular gyrus (Dice coefficient 0.24, Fig. 6B). PCA patients showed increased connectivity to left angular gyrus from both the medial pulvinar and DMN seeds, as well as increased connectivity to several voxels in the pregenual cingulate (Dice coefficient 0.14, Fig. 6C). There was little overlap between SN and lateral pulvinar-derived clusters (Dice coefficient 0.01, Fig. 6D). Widespread regions of diminished connectivity for PCA patients relative to HCs in parietooccipital cortex and insula were less prominent for either pulvinar seed compared with SN and DMN seeds.
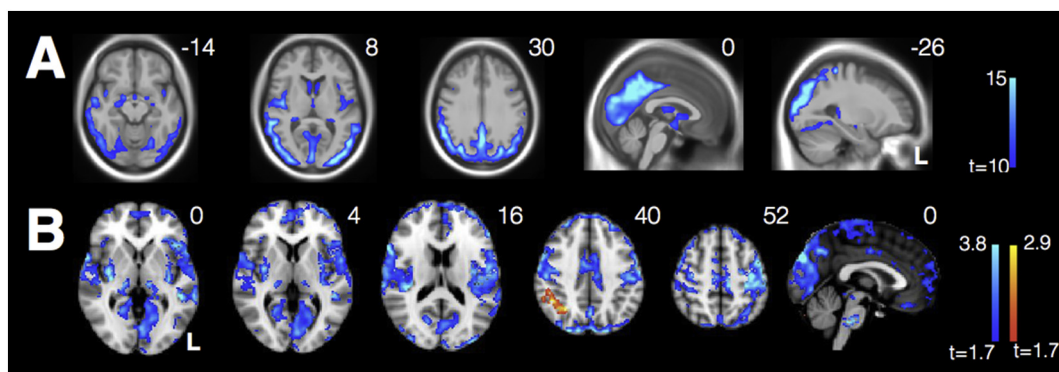
Fig. 4. (A) VBM reveals significant parietooccipital atrophy in individuals with PCA (threshold $t > 10$). Data are masked to gray matter and represent voxels where PCA patients show lower volume than HCs. (B) Decreased connectivity within the visuospatial network and from the R occipital seed to bilateral insula in PCAs compared with HCs. There is also increased connectivity between the seed and R angular gyrus in PCAs compared with HCs.

3.6. Regions of diminished visuospatial integrity in PCA do not correlate with neuropsychological performance; DMN integrity correlates with better short-term recall, while SN integrity correlates with increased IRI (personal distress)

We did not observe a significant relationship in PCA patients between VOSP score and visuospatial network integrity, represented by a parietooccipital cluster showing diminished connectivity from the visuospatial seed in PCA (Fig. 7, blue cluster). This was the case even when controlling for overall severity of illness (CDR sum-of-boxes) or general cognitive impairment (MMSE).

We did note a trend towards a correlation between short-term recall (CVLT long recall measure) and DMN integrity, represented by B angular gyrus clusters showing increased DMN connectivity in PCA (Fig. 7, red cluster), when controlling for general cognitive impairment ($r = 0.42, p = .07$). DMN integrity did not vary directly as a function of

either overall severity of illness of general cognitive impairment.

IRI performance related significantly to SN integrity. IRI (personal distress) correlated with connectivity from insula to mPFC, represented by mPFC cluster showing increased SN connectivity in PCA (Fig. 7, yellow cluster) in patients with PCA ($r = 0.47, p = .04$), such that increased connectivity was associated with increased personal distress. Conversely, IRI (empathic concern) correlated inversely with connectivity from insula to ventral striatum, represented by L ventral striatal cluster showing increased SN connectivity in PCA (Fig. 7, green cluster) in patients with PCA ($r = 0.36, p = .05$), such that increased connectivity was associated with decreased empathic concern.
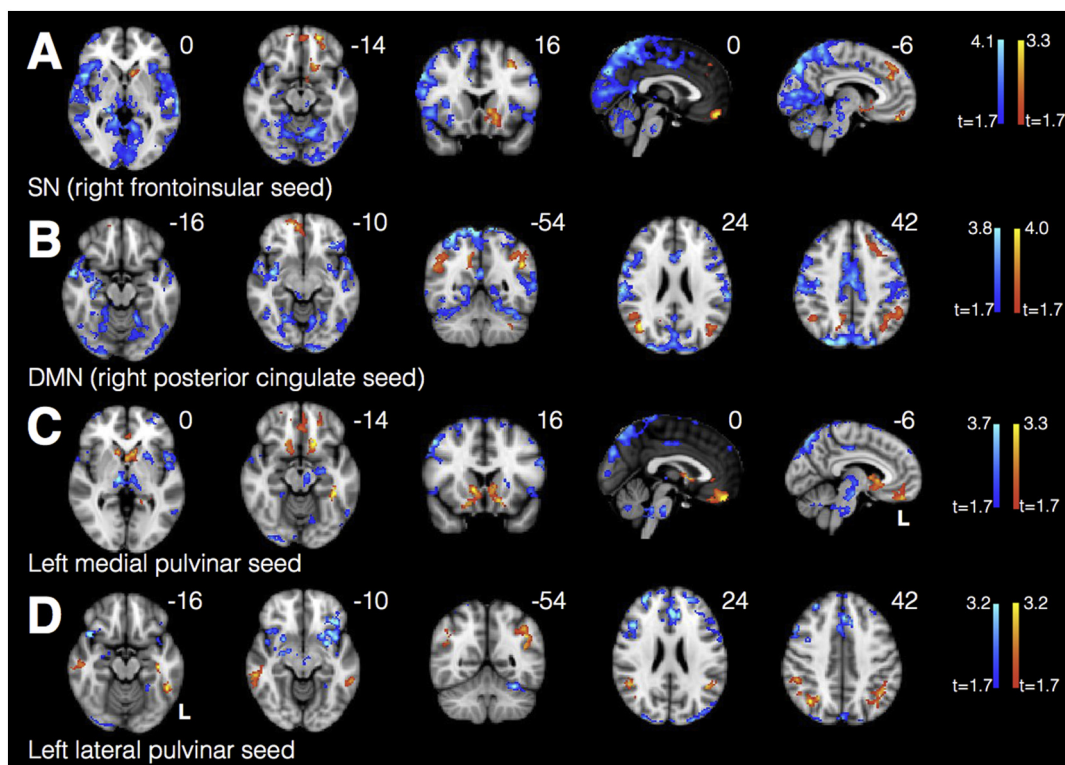

Fig. 5. PCA patients showed increased connectivity within key nodes of SN (A), DMN (B), medial pulvinar (C), and lateral pulvinar (D) compared to HCs. Warm colors represent areas of increased connectivity for PCA relative to HC; cool colors represent areas of decreased connectivity for PCA relative to HC.
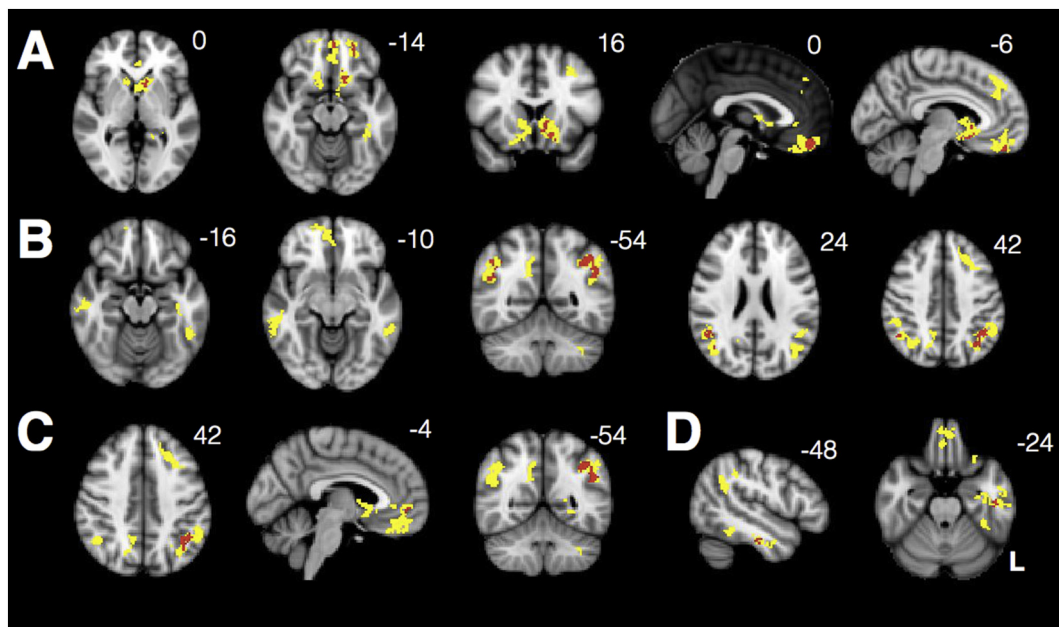
Fig. 6. Clusters shown represent the union of regions showing increased connectivity for PCA vs HC from (A) SN and medial pulvinar (Fig. 5A and C), (B) DMN and lateral pulvinar seeds (Fig. 5B and D), (C) DMN and medial pulvinar (Fig. 5B and C), and (D) SN and lateral pulvinar-seeded networks, with red areas representing the intersection. All maps were thresholded at a height by extent threshold of $p < .05$, $p < .05$ (corresponding to a Tmin of 1.7) prior to visualizing the union and intersection.

4. Discussion

4.1. Conclusions

Consistent with previous studies, our PCA sample show striking visuospatial processing impairments, accompanied by parietooccipital cortex atrophy and disrupted connectivity within a visuospatial network anchored by the lateral occipital gyrus, a point of peak atrophy in a prior PCA series (Ossenkoppele et al., 2015). The novel aspect of this study is our demonstration that patients with PCA score higher than HCs on measures of depressive symptomatology and personal distress, accompanied by preserved empathic concern and preserved to increased connectivity between key nodes of SN, which is thought to participate in social-emotional functioning. We further show that the
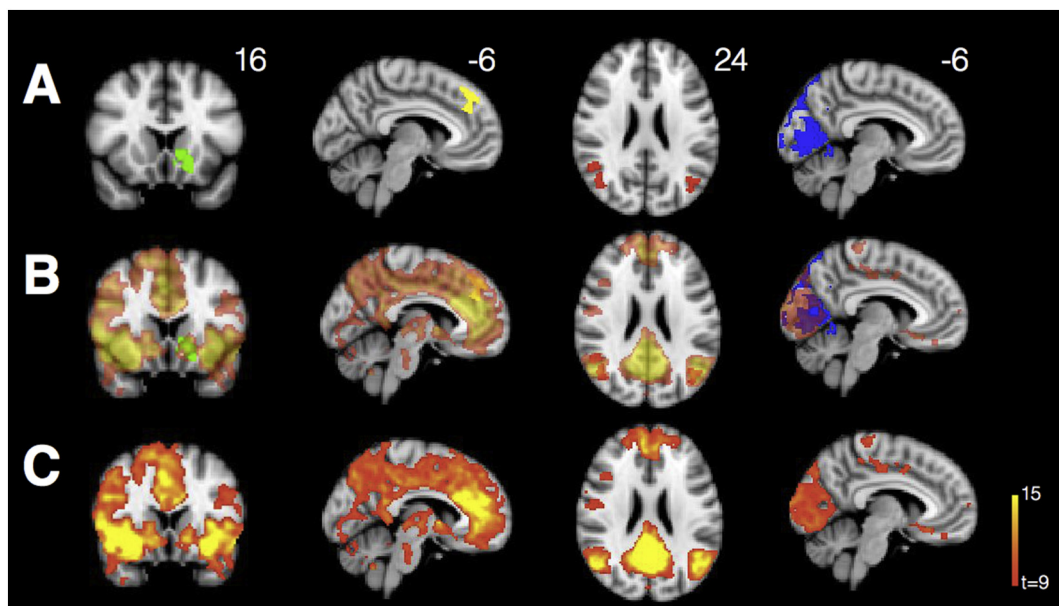

Fig. 7. Clusters extracted for neuropsychology-connectivity correlation analyses included (A) ventral striatal (green) and medial prefrontal (yellow) clusters whose connectivity to the SN seed was significantly increased for PCA relative to HCs; a bilateral angular gyrus cluster (red) whose connectivity to the DMN seed was significantly increased for PCA relative to HCs; and a parietooccipital cluster (blue) whose connectivity to the visuospatial network seed was significantly decreased for PCA relative to HCs. Clusters of interest are largely in-network for SN (first two columns), DMN (third column), and visuospatial network (fourth column). Transparent networks are shown overlaid on clusters of interest (B). We derive these networks using one-sample *t*-tests showing voxels correlating strongly with the R frontoinsula (SN), R posterior cingulate (DMN), and PCA peak atrophy (visuospatial network) seeds in a non-overlapping group of HCs (Supplemental Table 1) from that used for comparison with the PCA group (C).
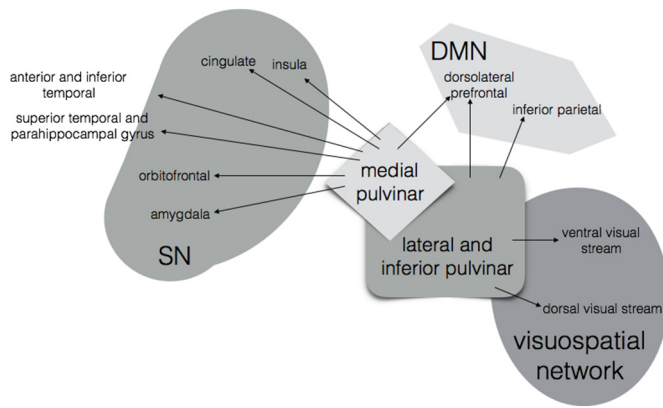
Fig. 8. Schematic illustrating anatomical connections between medial and lateral pulvinar and DMN, SN, and the visuospatial network (Benarroch, 2015; Robinson & Petersen, 1992; Yeterian & Pandya, 1995; Jones & Burton, 1976; Mufson & Mesulam, 1984; Romanski et al., 1997).

milder episodic memory deficits seen in PCA are accompanied by preserved to increased connectivity within the DMN. In addition, we suggest an as-yet-unexplored role for pulvinar thalamic subnuclei in PCA, showing that medial pulvinar connectivity is spatially similar to SN, while lateral pulvinar connectivity is similar to DMN.

Only one previous study evaluated network connectivity in PCA, focusing on differences between connectivity in PCA and other AD variants and showing that PCA patients show relative decreases in visuospatial network integrity (Lehmann et al., 2015). One past tractography study in PCA suggests damage to visual tracts including the bilateral inferior longitudinal fasciculus and left fronto-occcipital fasciculus (Migliaccio et al., 2012). Our findings are consistent with this work, showing decreased integrity of the visuospatial network in PCA relative to HCs.

Like individuals with amnestic AD (Sturm et al., 2013), the PCA patients in this study showed preserved empathic concern and increased personal distress and depressive symptoms relative to healthy controls. In keeping with these results, they also showed preserved to enhanced connectivity in the SN. Increased personal distress correlated with enhanced SN connectivity, similar to findings of enhanced SN connectivity associated with socioemotional sensitivity in amnestic and preclinical AD (Zhou et al., 2010; Balthazar et al., 2014; Fredericks et al., 2018). Insight into illness could play a contributing role in anxiety and depressive symptoms in PCA patients and in AD more generally. We found an association only between IRI measures (which focus on individuals' response to stressful external events) and SN connectivity, but there is also evidence that neuropsychiatric symptoms (which could reflect internal stress related to insight, among other things) and increased emotional reactivity (to both internal and external stressors, potentially) correlate with enhanced SN connectivity in amnestic and preclinical AD (Balthazar et al., 2014; Fredericks et al., 2018).

Unlike amnestic AD patients, however, PCA patients also showed preserved to enhanced connectivity between key nodes of the DMN, a network that plays a critical role in short-term memory. This was surprising, given PCA patients' profound atrophy in parietal regions that are critical nodes within this network. Specifically, we noted enhancements between the DMN seed and bilateral angular gyrus, ipsilateral precuneus, and anterior cingulate, while connectivity to ipsilateral hippocampus was decreased. Angular gyrus connectivity within the DMN correlated with higher short-term recall when controlling for general cognitive impairment, and angular gyrus connectivity was enhanced in PCA across multiple other networks, suggesting that the angular gyrus might be playing a specific role in preserving short-term memory performance relative to global cognitive functioning. More generally, enhanced connectivity both within the DMN and across

networks in PCA may represent a compensatory mechanism supporting the relative preservation of non-visuospatial cognition.

Prior studies of patients with amnestic AD show early decreases in DMN integrity accompanied by increases in connectivity within SN, while patients with behavioral variant frontotemporal dementia show the opposite pattern, with decreases in SN connectivity accompanied by relative increases in DMN (Zhou et al., 2010; Rabinovici et al., 2007; Seeley et al., 2007). In our PCA population, we observed decreases in visuospatial network connectivity accompanied by enhancements within both DMN and SN. What could be driving this reciprocal relationship?

Thalamic nuclei are well-positioned to coordinate within-network activity and to regulate switching between networks (Hwang et al., 2017; Bell & Shine, 2016; Sherman, 2016), and previous graph theoretical analyses on "rich-club" organization within the human brain pinpoints the thalamus as one of twelve hubs which shows particularly dense interconnectivity, even beyond what would be expected based on its nodal degree (van den Heuvel & Sporns, 2011). An emerging animal literature links thalamic pathology to increased excitability in thalamic relay nuclei, sleep disturbance, and hippocampal dysfunction in models of AD (Hazra et al., 2016). Specific thalamic nuclei are implicated in specific subtypes of AD. For instance, the anterior nucleus is affected very early in the course of amnestic AD, representing one of the earliest sites of forebrain tau accumulation, with involvement tracking alongside that of the hippocampus (Braak & Braak, 1991; Rub et al., 2016). It plays a critical role in associative memory performance as part of the Papez circuit (Aggleton & Brown, 1999; Fama & Sullivan, 2015), and has direct links to both hippocampus and posterior cingulate (Amaral & Cowan, 1980; Vogt et al., 1987; Aggleton et al., 1986), two key nodes of the DMN, which shows progressive dysfunction in amnestic AD (Zhou et al., 2010; Greicius et al., 2004; Damoiseaux et al., 2012). A direct electrophysiological study has shown that anterior thalamic synchrony with neocortex predicts memory performance (Sweeney-Reed et al., 2015). Despite these promising inroads, and despite the early involvement of the anterior thalamus in amnestic AD pathophysiology, the role of thalamic nuclei in AD remains understudied.

The pulvinar nuclei of the thalamus are of particular interest in PCA given their strong anatomical connections to regions in the visuospatial network, SN, and DMN (Fig. 8). The lateral pulvinar has direct projections to cortical regions in striate cortex and along the dorsal and ventral visual streams, as well as to the inferior parietal lobe and the dorsolateral prefrontal cortex, sites of key nodes within the DMN (Benarroch, 2015; Robinson & Petersen, 1992; Yeterian & Pandya, 1995). The medial pulvinar has similarly prominent reciprocal connections with major nodes of SN, including orbitofrontal, parahippocampal, cingulate, insular and amygdalar regions (Benarroch, 2015; Jones & Burton, 1976; Mufson & Mesulam, 1984; Romanski et al., 1997), as well as frontal DMN nodes. In amnestic AD, amyloid plaques aggregate in the pulvinar nucleus and its adjacent fiber tract, the pulvinar capsule (Leuba & Saini, 1995; Kuljis, 1994), and one study of preclinical AD patients showed a negative correlation between CSF tau and cerebral glucose metabolism in key regions of the DMN, including PCC, precuneus, and parahippocampal gyrus – as well as in the pulvinar (Petrie et al., 2009). Atrophy in the medial pulvinar has previously been associated with decreased SN connectivity in patients with one genetic form of behavioral variant FTD (Lee et al., 2014).

In this study, lateral pulvinar connectivity to major DMN nodes was increased in PCA patients in a pattern similar to that elicited by the DMN seed, though with the addition of the parahippocampal gyrus. Lateral pulvinar connectivity to some parietal and occipital clusters was decreased, though not to the extent seen in the visuospatial network. Medial pulvinar connectivity to nucleus accumbens and ventral prefrontal cortex was increased in PCA patients in a pattern similar to that elicited by the SN seed. Though our work cannot assess for a moderating effect of pulvinar nuclei on network integrity, our findings are consistent with a model of PCA in which thalamic nuclei and their

reciprocal cortical connections help to bind heavily impacted cortical regions with relatively less affected regions that participate in the same functional networks. The widespread cortical projections of both the medial and lateral pulvinar nuclei may position them well to coordinate compensatory shifts across networks, allowing for relative preservation of non-visuospatial cognitive functions well into the course of illness.

4.2. Limitations and future directions

Our exploratory post-hoc analyses were not able to find a relationship between visuospatial task performance and visuospatial network integrity in PCA. This may have been due in part to clinical and radiographic heterogeneity within the PCA population, or simply due to low power given our relatively small sample size. However, we identified a weak correlation between enhanced DMN connectivity and higher short-term recall in PCA patients. We also found a correlation between increased SN connectivity (between the right frontoinsular seed and a medial prefrontal cluster) and the IRI measure of personal distress in PCA patients, and a negative correlation between frontoinsular and ventral striatum connectivity and the IRI measure of empathic concern. These findings suggest that enhanced SN connectivity may underlie the heightened personal distress seen in our PCA group, but that PCA patients' preserved empathic concern arises by some other mechanism. Future studies targeted at understanding the relationship between neuropsychological task performance and network integrity should help clarify the means by which changes in large-scale functional networks underlie variations in performance on specific neuropsychological tasks in both patient and healthy populations.

The data we present here are consistent with a role for specific thalamic nuclei in network dysfunction in the PCA variant of AD. Specifically, the similarity of the lateral pulvinar-derived connectivity map to the DMN-seeded map, and of the medial pulvinar-derived map to SN-seeded map, suggests an important role for the pulvinar within these networks, and reflects the close anatomical relationship between medial pulvinar and SN, and lateral pulvinar and DMN and visuospatial regions. Because the functional connectivity methods employed here are based on region-to-region correlations in BOLD signal, they cannot assess directionality. What role do thalamic nuclei play in facilitating information transfer and network switching in health and in AD? Future work will be critical to better understand the role of the pulvinar in PCA, and, more generally, the role of specific thalamic subnuclei in network modulation in the healthy brain and clinical AD variants. Pathological studies which better specify the involvement of the pulvinar in AD and in PCA in particular, high-field imaging at the thalamic nuclear level assessing microstructural changes in vivo, partial correlation analyses assessing for the unique contribution of thalamic nuclei to connectivity networks, and studies that evaluate task-related output from thalamic subnuclei and their relationship to networks known to be critically impacted in AD will add to our understanding.

Supplementary data to this article can be found online at https://doi.org/10.1016/j.nicl.2018.101628.

Acknowledgements

References

409–421.

Amaral, D.G., Cowan, W.M., 1980. Subcortical afferents to the hippocampal formation in the monkey. J. Comp. Neurol. 189 (4), 573–591.

Armstrong, M.J., Litvan, I., Lang, A.E., Bak, T.H., Bhatia, K.P., Borroni, B., et al., 2013. Criteria for the diagnosis of corticobasal degeneration. Neurology 80 (5), 496–503.

Balthazar, M.L., Pereira, F.R., Lopes, T.M., da Silva, E.L., Coan, A.C., Campos, B.M., et al., 2014. Neuropsychiatric symptoms in Alzheimer's disease are related to functional connectivity alterations in the salience network. Hum. Brain Mapp. 35 (4), 1237–1246.

Bell, P.T., Shine, J.M., 2016. Subcortical contributions to large-scale network communication. Neurosci. Biobehav. Rev. 71, 313–322.

Benarroch, E.E., 2015. Pulvinar: associative role in cortical function and clinical correlations. Neurology 84 (7), 738–747.

Benson, D.F., Davis, R.J., Snyder, B.D., 1988. Posterior cortical atrophy. Arch. Neurol. 45 (7), 789–793.

Braak, H., Braak, E., 1991. Neuropathological staging of Alzheimer-related changes. Acta Neuropathol. 82 (4), 239–259.

Casanova, R., Srikanth, R., Baer, A., Laurienti, P.J., Burdette, J.H., Hayasaka, S., et al., 2007. Biological parametric mapping: a statistical toolbox for multimodality brain image analysis. NeuroImage 34 (1), 137–143.

Crutch, S.J., Schott, J.M., Rabinovici, G.D., Murray, M., Snowden, J.S., van der Flier, W.M., et al., 2017. Consensus classification of posterior cortical atrophy. Alzheimers Dement. 13 (8), 870–884.

Damoiseaux, J.S., Prater, K.E., Miller, B.L., Greicius, M.D., 2012. Functional connectivity tracks clinical deterioration in Alzheimer's disease. Neurobiol. Aging 33 (4), 828 e19–30.

Davis, M.H., 1983. Measuring individual differences in empathy: evidence for a multidimensional approach. J. Pers. Soc. Psychol. 44 (1).

Delis, D.C., Kramer, J.H., Kaplan, E., Ober, B.A., 2000. California Verbal Learning Test, 2 ed. The Psychological Corporation, San Antonio, TX.

Fama, R., Sullivan, E.V., 2015. Thalamic structures and associated cognitive functions: Relations with age and aging. Neurosci. Biobehav. Rev. 54, 29–37.

Folstein, M.F., Folstein, S.E., McHugh, P.R., 1975. Mini-mental state. A practical method for grading the cognitive state of patients for the clinician. J. Psychiatr. Res. 12 (3), 189–198.

Fredericks, C.A., Sturm, V.E., Brown, J.A., Hua, A.Y., Bilgel, M., Wong, D.F., et al., 2018. Early affective changes and increased connectivity in preclinical Alzheimer's disease. Alzheimers Dement (Amst). 10, 471–479.

Gardner, R.C., Boxer, A.L., Trujillo, A., Mirsky, J.B., Guo, C.C., Gennatas, E.D., et al., 2013. Intrinsic connectivity network disruption in progressive supranuclear palsy. Ann. Neurol. 73 (5), 603–616.

Greicius, M.D., Srivastava, G., Reiss, A.L., Menon, V., 2004. Default-mode network activity distinguishes Alzheimer's disease from healthy aging: evidence from functional MRI. Proc. Natl. Acad. Sci. U. S. A. 101 (13), 4637–4642.

Guo, C.C., Kurth, F., Zhou, J., Mayer, E.A., Eickhoff, S.B., Kramer, J.H., et al., 2012. One-year test-retest reliability of intrinsic connectivity network fMRI in older adults. NeuroImage 61 (4), 1471–1483.

Hazra, A., Corbett, B.F., You, J.C., Aschmies, S., Zhao, L., Li, K., et al., 2016. Corticothalamic network dysfunction and behavioral deficits in a mouse model of Alzheimer's disease. Neurobiol. Aging 44, 96–107.

Hof, P.R., Archin, N., Osmand, A.P., Dougherty, J.H., Wells, C., Bouras, C., et al., 1993. Posterior cortical atrophy in Alzheimer's disease: analysis of a new case and re-evaluation of a historical report. Acta Neuropathol. 86 (3), 215–223.

Hwang, K., Bertolero, M.A., Liu, W.B., D'Esposito, M., 2017. The human thalamus is an integrative hub for functional brain networks. J. Neurosci. 37 (23), 5594–5607.

Isella, V., Villa, G., Mapelli, C., Ferri, F., Appollonio, I.M., Ferrarese, C., 2015. The neuropsychiatric profile of posterior cortical atrophy. J. Geriatr. Psychiatry Neurol. 28 (2), 136–144.

Jones, E.G., Burton, H., 1976. A projection from the medial pulvinar to the amygdala in primates. Brain Res. 104 (1), 142–147.

Krauth, A., Blanc, R., Poveda, A., Jeanmonod, D., Morel, A., Szekely, G., 2010. A mean three-dimensional atlas of the human thalamus: generation from multiple histological data. NeuroImage 49 (3), 2053–2062.

Kuljis, R.O., 1994. Lesions in the Pulvinar in patients with Alzheimers-Disease. J. Neuropathol. Exp. Neurol. 53 (2), 202–211.

Lee, S.E., Khazenzon, A.M., Trujillo, A.J., Guo, C.C., Yokoyama, J.S., Sha, S.J., et al., 2014. Altered network connectivity in frontotemporal dementia with C9orf72 hexanucleotide repeat expansion. Brain J. Neurol. 137, 3047–3060.

Lehmann, M., Madison, C.M., Ghosh, P.M., Seeley, W.W., Mormino, E., Greicius, M.D., et al., 2013. Intrinsic connectivity networks in healthy subjects explain clinical variability in Alzheimer's disease. Proc. Natl. Acad. Sci. U. S. A. 110 (28), 11606–11611.

Lehmann, M., Madison, C., Ghosh, P.M., Miller, Z.A., Greicius, M.D., Kramer, J.H., et al., 2015. Loss of functional connectivity is greater outside the default mode network in nonfamilial early-onset Alzheimer's disease variants. Neurobiol. Aging 36 (10), 2678–2686.

Leuba, G., Saini, K., 1995. Pathology of subcortical visual centers in relation to cortical degeneration in alzheimers-disease. Neuropathol. Appl. Neurobiol. 21 (5), 410–422.

Mack, W.J., Freed, D.M., Williams, B.W., Henderson, V.W., 1992. Boston naming test: shortened versions for use in alzheimer's disease. J. Gerontol. 47 (3), P154–P158.

McKeith, I.G., Boeve, B.F., Dickson, D.W., Halliday, G., Taylor, J.P., Weintraub, D., et al., 2017. Diagnosis and management of dementia with Lewy bodies: fourth consensus report of the DLB Consortium. Neurology 89 (1), 88–100.

Mendez, M.F., Ghajarania, M., Perryman, K.M., 2002. Posterior cortical atrophy: clinical characteristics and differences compared to Alzheimer's disease. Dement. Geriatr. Cogn. Disord. 14 (1), 33–40.

Aggleton, J.P., Brown, M.W., 1999. Episodic memory, amnesia, and the hippocampal-anterior thalamic axis. Behav. Brain Sci. 22 (3), 425–444 (discussion 44-89).

Aggleton, J.P., Desimone, R., Mishkin, M., 1986. The origin, course, and termination of the hippocampothalamic projections in the macaque. J. Comp. Neurol. 243 (3),

Migliaccio, R., Agosta, F., Scola, E., Magnani, G., Cappa, S.F., Pagani, E., et al., 2012. Ventral and dorsal visual streams in posterior cortical atrophy: a DT MRI study. Neurobiol. Aging 33 (11), 2572–2584.

Mormino, E.C., Smiljic, A., Hayenga, A.O., Onami, S.H., Greicius, M.D., Rabinovici, G.D., et al., 2011. Relationships between beta-amyloid and functional connectivity in different components of the default mode network in aging. Cereb. Cortex 21 (10), 2399–2407.

Mufson, E.J., Mesulam, M.M., 1984. Thalamic connections of the insula in the rhesus monkey and comments on the paralimbic connectivity of the medial pulvinar nucleus. J. Comp. Neurol. 227 (1), 109–120.

Ossenkoppele, R., Cohn-Sheehy, B.I., La Joie, R., Vogel, J.W., Moller, C., Lehmann, M., et al., 2015. Atrophy patterns in early clinical stages across distinct phenotypes of Alzheimer's disease. Hum. Brain Mapp. 36 (11), 4421–4437.

Petrie, E.C., Cross, D.J., Galasko, D., Schellenberg, G.D., Raskind, M.A., Peskind, E.R., et al., 2009. Preclinical evidence of Alzheimer changes: convergent cerebrospinal fluid biomarker and fluorodeoxyglucose positron emission tomography findings. Arch. Neurol. 66 (5), 632–637.

Possin, K.L., Laluz, V.R., Alcantar, O.Z., Miller, B.L., Kramer, J.H., 2011. Distinct neuroanatomical substrates and cognitive mechanisms of figure copy performance in Alzheimer's disease and behavioral variant frontotemporal dementia. Neuropsychologia 49 (1), 43–48.

Rabinovici, G.D., Seeley, W.W., Kim, E.J., Gorno-Tempini, M.L., Rascovsky, K., Pagliaro, T.A., et al., 2007. Distinct MRI atrophy patterns in autopsy-proven Alzheimer's disease and frontotemporal lobar degeneration. Am J Alzheimers Dis Other Demen. 22 (6), 474–488.

Robinson, D.L., Petersen, S.E., 1992. The pulvinar and visual salience. Trends Neurosci. 15 (4), 127–132.

Romanski, L.M., Giguere, M., Bates, J.F., Goldman-Rakic, P.S., 1997. Topographic organization of medial pulvinar connections with the prefrontal cortex in the rhesus monkey. J. Comp. Neurol. 379 (3), 313–332.

Rub, U., Stratmann, K., Heinsen, H., Del Turco, D., Ghebremedhin, E., Seidel, K., et al., 2016. Hierarchical distribution of the tau cytoskeletal pathology in the thalamus of alzheimer's disease patients. J. Alzheimers Dis. 49 (4), 905–915.

Satterthwaite, T.D., Elliott, M.A., Gerraty, R.T., Ruparel, K., Loughead, J., Calkins, M.E., et al., 2013. An improved framework for confound regression and filtering for control of motion artifact in the preprocessing of resting-state functional connectivity data. NeuroImage 64, 240–256.

Seeley, W.W., Allman, J.M., Carlin, D.A., Crawford, R.K., Macedo, M.N., Greicius, M.D., et al., 2007. Divergent social functioning in behavioral variant frontotemporal dementia and Alzheimer disease: reciprocal networks and neuronal evolution. Alzheimer Dis. Assoc. Disord. 21 (4), S50–S57.

Seeley, W.W., Zhou, J., Kim, E.J., 2012. Frontotemporal dementia: what can the behavioral variant teach us about human brain organization? Neuroscientist 18 (4), 373–385.

Sherman, S.M., 2016. Thalamus plays a central role in ongoing cortical functioning. Nat. Neurosci. 19 (4), 533–541.

Spreen, O., Strauss, E., 1998. A Compendium of Neuropsychological Tests: Administration, Norms, and Commentary. Oxford University Press, Oxford, UK.

Sturm, V.E., Yokoyama, J.S., Seeley, W.W., Kramer, J.H., Miller, B.L., Rankin, K.P., 2013. Heightened emotional contagion in mild cognitive impairment and Alzheimer's disease is associated with temporal lobe degeneration. Proc. Natl. Acad. Sci. U. S. A. 110 (24), 9944–9949.

Sweeney-Reed, C.M., Zaehle, T., Voges, J., Schmitt, F.C., Buentjen, L., Kopitzki, K., et al., 2015. Thalamic theta phase alignment predicts human memory formation and anterior thalamic cross-frequency coupling. elife 4.

Tang-Wai, D.F., Graff-Radford, N.R., Boeve, B.F., Dickson, D.W., Parisi, J.E., Crook, R., et al., 2004. Clinical, genetic, and neuropathologic characteristics of posterior cortical atrophy. Neurology 63 (7), 1168–1174.

van den Heuvel, M.P., Sporns, O., 2011. Rich-club organization of the human connectome. J. Neurosci. 31 (44), 15775–15786.

Vogt, B.A., Pandya, D.N., Rosene, D.L., 1987. Cingulate cortex of the rhesus monkey: I. Cytoarchitecture and thalamic afferents. J. Comp. Neurol. 262 (2), 256–270.

Warrington, E.K.J., 1991. The Visual Object and Space Perception Battery. Bury St Edmunds. Thames Valley Test Company, England.

Weintraub, S., Salmon, D., Mercaldo, N., Ferris, S., Graff-Radford, N.R., Chui, H., et al., 2009. The Alzheimer's Disease Centers' Uniform Data Set (UDS): the neuropsychologic test battery. Alzheimer Dis. Assoc. Disord. 23 (2), 91–101.

Weschler, D., 1987. Weschler Memory Scale — Revised. The Psychological Corporation, San Antonio.

Yeo, B.T., Krienen, F.M., Sepulcre, J., Sabuncu, M.R., Lashkari, D., Hollinshead, M., et al., 2011. The organization of the human cerebral cortex estimated by intrinsic functional connectivity. J. Neurophysiol. 106 (3), 1125–1165.

Yesavage, J.A., Brink, T.L., Rose, T.L., Lum, O., Huang, V., Adey, M., et al., 1982. Development and validation of a geriatric depression screening scale: a preliminary report. J. Psychiatr. Res. 17 (1), 37–49.

Yeterian, E.H., Pandya, D.N., 1995. Corticostriatal connections of extrastriate visual areas in rhesus monkeys. J. Comp. Neurol. 352 (3), 436–457.

Zhou, J., Greicius, M.D., Gennatas, E.D., Growdon, M.E., Jang, J.Y., Rabinovici, G.D., et al., 2010. Divergent network connectivity changes in behavioural variant frontotemporal dementia and Alzheimer's disease. Brain J. Neurol. 133, 1352–1367 Pt 5.